Proceedings of the 21st ICSMGE, Vienna, Austria, 14 – 19 June 2026. Pistrol, Adam & Schweiger (eds.)
Published by: ÖGG, Austrian Society for Geomechanics, Salzburg, Austria, ISBN 978-3-9503898-4-5
https://doi.org/10.53243/ICSMGE2026-1932

Fragility and functionality loss curves of geotechnical systems in road infrastructures

Filomena de Silva, Francesco Dionisio, Valeria Abbatiello, Francesco Silvestri
Università degli Studi di Napoli "Federico II", Napoli, Italia. filomena.desilva@unina.it

Chiara Amendola
Aristotele University of Thessaloniki, Thessaloniki, Greece

Riccardo Conti
Università degli Studi di Roma "Tor Vergata", Roma, Italia

ABSTRACT: Retaining walls and embankments are frequently used to support road and railway infrastructure systems. An adequate assessment of the seismic performance of these systems is of fundamental importance both to assess the loss of functionality of the network after a seismic event and to plan maintenance interventions on infrastructures. Seismic performance can be evaluated following a probabilistic approach, based on the construction of fragility curves, which provide the probability that the seismic demand exceeds the capacity of the system, conditional on a given level of seismic shaking. In the case of retaining structures, these curves are typically obtained for particular case studies and, therefore, difficult to generalize to the variety of systems along the networks. This work presents sets of fragility curves obtained for retaining walls and road embankments as part of the PRIN PNRR 2022 "*Framework to Assess Infrastructure Resilience and Management Operations In Roads After Earthquake*". Thousands of nonlinear dynamic analyses were performed, varying the seismic inputs, the structural geometry, and the critical acceleration values. The results, validated through comparison with four case studies, were used to define generalized fragility curves applicable to all retaining walls and embankments.

KEYWORDS: retaining walls, embankments, fragility curves, infrastructure resilience.

1 INTRODUCTION

A study published by the World Bank Group in 2019 highlighted that approximately 27% of the world's road infrastructure is exposed to potentially catastrophic natural events, including earthquakes. The sudden loss of functionality of such infrastructures following an earthquake can severely hinder emergency response operations, thereby increasing both the number of casualties and the associated economic losses, ultimately amplifying the overall seismic risk.

The operational efficiency of the road network in the immediate post-earthquake phase critically depends on the performance of its structural and geotechnical components. It is therefore essential to have risk assessment tools at the territorial scale, which are useful both for planning pre-event mitigation measures and for defining post-event intervention priorities. One of the most commonly used tools for this purpose is the fragility curves, which provide an estimate of the probability of exceeding various damage states as a function of a seismic intensity measure. This estimate is based on the comparison between the demand parameter and thresholds representative of different damage levels. In the following, this approach is applied to retaining walls supporting roads and embankments along the Italian highway network.

2 METHOD OF ANALYSIS

The aim of this study is to develop analytical tools to quantify the functionality loss of the Italian road infrastructure due to seismic damage to retaining walls and embankments. Since discontinuities on the road surface are the main factor compromising safe usability, the most effective damage parameter is the permanent vertical displacement, v_{res}, classified according to the damage scale proposed by Kaynia *et al.* (2011), *i.e.*: DS_1 is reached if v_{res} = 0.05 m ± 0.03 m, DS_2 if v_{res} = 0.15 m ± 0.07 m, and DS_3 if v_{res} = 0.44 m ± 0.18 m. Earthquake-induced permanent vertical displacements are a consequence of the onset of horizontal sliding or wall rotation, or of instability mechanisms in embankments. Numerical analyses by Cosentini and Bozzoni (2022) have shown that sliding mechanisms maximize the fragility of retaining walls. Similarly, the high mechanical properties required for foundation soils and the drained conditions typical of well-constructed embankments make sliding along a logarithmic spiral failure surface the most likely collapse mechanism for road embankments. In those cases, the estimation of expected damage to a wall or an embankment is effectively an analysis of its sliding response.

To obtain generalizable results, many analyses on different prototypes must be performed. An efficient way to quantify displacement is through linear dynamic analysis, where the residual horizontal displacement u_{res} is calculated as the double integral of the relative acceleration of the wall or embankment, when the applied accelerogram exceeds a threshold acceleration. In this study, the threshold increases with displacement according to the so-called capacity curve, up to a plateau corresponding to the well-known critical acceleration, a_c.

A total of 177 ground motion records were considered in this study, all recorded during real events at stations located on soil types A, B, C, and D, as classified by the Italian technical code for constructions. This approach, known as the Cloud Method, allows to analyze the effect on the performance of the different seismic amplitude and frequency contents expected to occur in different soil types, avoiding the unrealistic modifications introduced by scaling the input motions (Jalayer et al., 2015).

The computed residual horizontal displacements were plotted in a bi-logarithmic plane against the ratio of the peak ground acceleration to the critical acceleration of the wall, a_{max}/a_c. The data were interpolated using linear regression to derive the following equation:

$$\ln(u_{res}) = \ln(a) + b \ln\left(\frac{a_{max}}{a_c}\right) \quad (1a)$$

characterized by a standard deviation:

$$\beta_{EDP} = \frac{\sqrt{\sum_{i=1}^{n}[\ln(u_{res})^* - \ln(u_{res})]_i^2}}{\sqrt{n-2}} \quad (1b)$$

where ln(a) and b are the regression parameters, a_{max} is the peak ground acceleration, ln(u_{res})* is the numerical results and ln(u_{res}) is the prediction of Eq.(1a) for the a_{max}/a_c leading to ln(u_{res})* and n is the number of the executed seismic analyses.

As typical in fragility analyses through the cloud method (Jalayer et al., 2015), the residual horizontal displacement is assumed to follow a lognormal distribution with mean value μ_{lnEDP} and standard deviation β_{EDP}, the probability of exceedance of the i-th damage state DS_i can be estimated as follows:

$$P(DSi) = \Phi\left[-\frac{DSi - \mu_{lnEDP}}{\sqrt{\beta_{EDP}^2 + \beta_C^2}}\right] \quad (2)$$

where:

- DS_i is the damage threshold expressed in terms of residual horizontal displacement (i.e.: 0.05 m, 0.15 m, and 0.4 m), as inferred from the vertical displacement thresholds by Kaynia et al. (2011);
- β_C represents the uncertainty related to the capacity model, assumed as 0.3b (NIBS, 1999);
- μ_{lnEDP} corresponds to ln(u_{res}) obtained from Eq.(1a), and β_{EDP} is derived from Eq.(1b).

The exceedance of each DSi can be associated with a level of functionality loss FL_i, representing an action aimed at ensuring road user safety. FL_i is considered reached when the corresponding DSi exceeds a threshold value. The threshold was set to 10% in this study, but whatever different value can be chosen by decision makers. In this way, fragility curves can be directly converted into functionality loss functions, as follows:

- FL_1, associated with $P(DS1) > 10\%$, implies speed reduction;
- FL_2, associated with $P(DS2) > 10\%$, implies speed reduction and partial or full lane closure;
- FL_3, associated with $P(DS3) > 10\%$, implies full road closure.

3 EMBANKMENTS AND WALLS SUPPORTING HIGHWAY ITALIAN ROADS

A statistical analysis of the data provided by *Autostrade per l'Italia S.p.A.* revealed the most common geometric characteristics of embankments and retaining walls, as shown in Figure 1 and Figure 2.

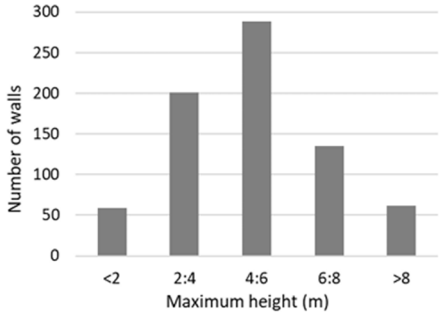

Figure 1. Geometric characteristics of retaining walls on the Italian highway network.

For embankments, only cases with available geotechnical characterization were considered. In particular, the heights of retaining walls are generally between 2 m and 8 m, while embankments can reach heights up to 18 m, with the maximum slope increasing with height.

Based on this evidence, linear dynamic analyses were carried out on retaining walls with heights of 2, 4, 6, and 8 m, considering typical values of a_c equal to 0.05, 0.1, 0.2, and 0.3 g. For each configuration, capacity curves were constructed following the model proposed by Callisto (2019), assuming a yield displacement equal to 0.7% of the wall height and a ratio between the critical acceleration and the asymptotic value of the hyperbolic function equal to 0.7. The resulting curves are shown in Figure 3.

From the embankment envelope in Figure 2, the configurations marked with cross- and x-shaped indicators were selected. These were characterized by mechanical properties representative of coarse-grained and fine-grained soils, as reported in Table 1, based on the most common characteristics.

For each of the 21 configurations, finite difference models were developed using the FLAC2D code, and capacity curves were obtained by calculating the displacement of the top of the embankment for increasing values of horizontal acceleration uniformly applied to the model. The results were interpreted using a hyperbolic model to derive the curves shown in Figure 4. Curves associated with more than one embankment were derived by interpolating all results when they were closely spaced.

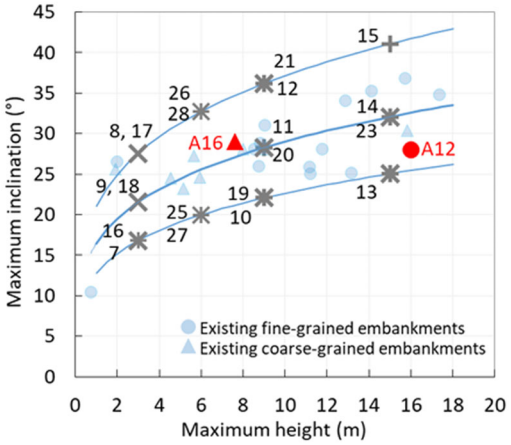

Figure 2. Geometric characteristics of embankments on the Italian highway network. The grey symbols indicate the geometric features of the analyzed embankment, considered made of fine grained (x), coarse grained (+) soil models and both soil models (*).

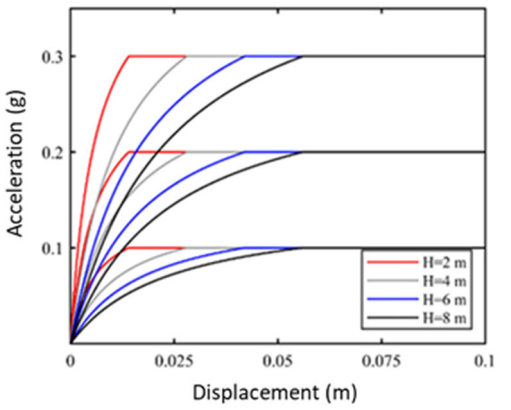

Figure 3. Capacity curves adopted in the analysis of retaining walls.

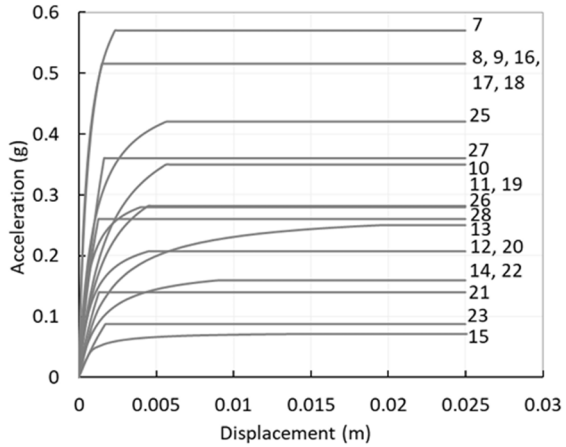

Figure 4. Capacity curves adopted in the analysis of embankments. The number on the right side of each curve refers to the embankment geometric features in Figure 2.

Table 1. Mechanical properties of embankments

Parameters of coarse-grained soils (Embankments 7,8,9,10,11,12,13,14,15,25,26)	Symbol	Value	Unit
Unit weight	γ	18	KN/m^3
Cohesion	c	5	KPa
Friction angle	φ	35	°
Shear wave velocity	V_s	250	m/s
Shear modulus	*G*	114.7	MPa
Poisson's ratio	*v*	0.3	-
Bulk modulus	*K*	248.5	MPa

Parameters of fine-grained soils (Embankments 16,17,18,19,20,21,22,23,27,28)	Symbol	Value	Unit
Unit weight	γ	20	KN/m^3
Cohesion	c	10	KPa
Friction angle	φ	25	°
Shear wave velocity	V_s	250	m/s
Shear modulus	*G*	127.4	MPa
Poisson's ratio	*v*	0.4	-
Bulk modulus	*K*	594.6	MPa

4 RESULTS

The resulting displacements for embankments show limited sensitivity to height and slope near the damage thresholds (see Figure 5).

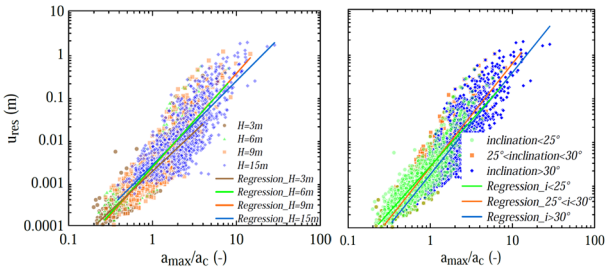

Figure 5. Displacement vs a_{max}/a_c data in relation to height and slope inclination.

This occurs because these thresholds fall within the plateau of the capacity curves, which depend solely on the critical acceleration of the embankment, used here to normalize the seismic intensity measure. On the other hand, a dependence on the soil type of the input motions remains (see Figure 6).

A similar result is observed for retaining walls (see Figure 7). For this reason, the fragility curves have been differentiated based on the ground type of seismic input, as shown in Figure 8. The parameters of the regression laws used to calculate the fragility curves through Equations (1a) and (1b) are listed in Table 2.

Table 2. Parameters of the regression laws

Embankment parameters	Symbol	Soil A	Soil B	Soil C	Soil D
Intercept parameter	a	0.0022	0.0019	0.0028	0.0020
Slope parameter	b	1.992	1.796	2.334	1.938
Standard deviation of the residuals	β_{EDP}	0.701	0.701	0.703	0.748

Retaining walls parameters	Symbol	Soil A	Soil B	Soil C	Soil D
Intercept parameter	a	0.021	0.016	0.021	0.017
Slope parameter	b	1.655	1.447	1.684	1.561
Standard deviation of the residuals	β_{EDP}	0.730	0.779	0.848	0.804

Alternatively, the results can be interpreted collectively using the so-called vector-based approach, in which more than one seismic intensity measure is considered. This approach has been applied to retaining walls by Amendola et al. (2025).

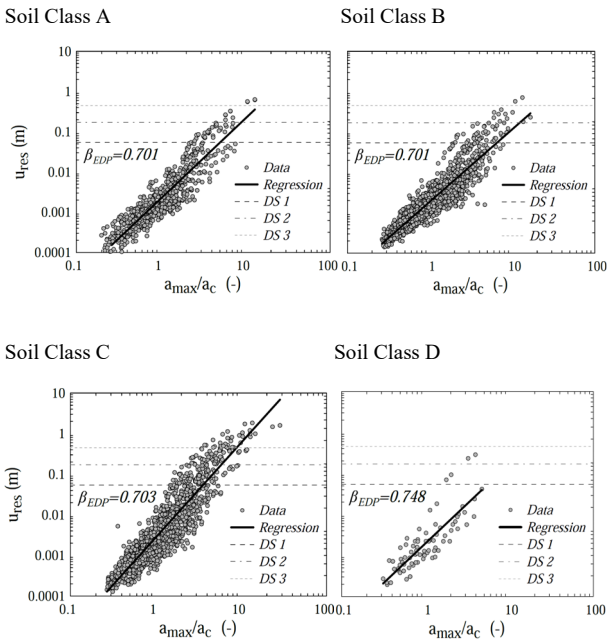

Figure 6. Displacement vs a_{max}/a_c data for soil types A, B, C, and D for embankments.

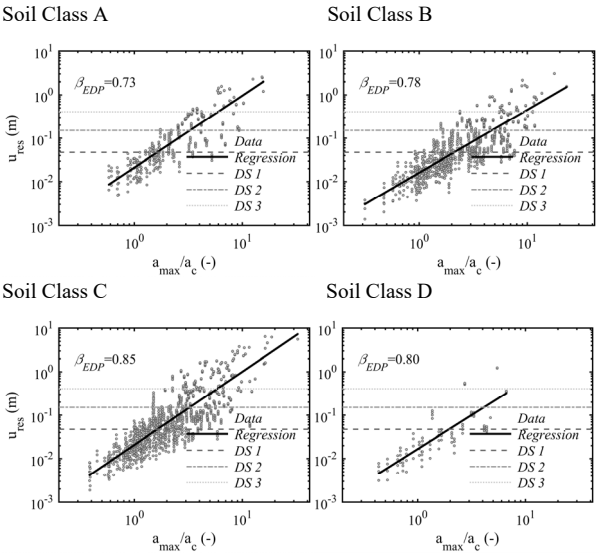

Figure 7. Displacement vs a_{max}/a_c data for soil types A, B, C, and D for retaining walls.

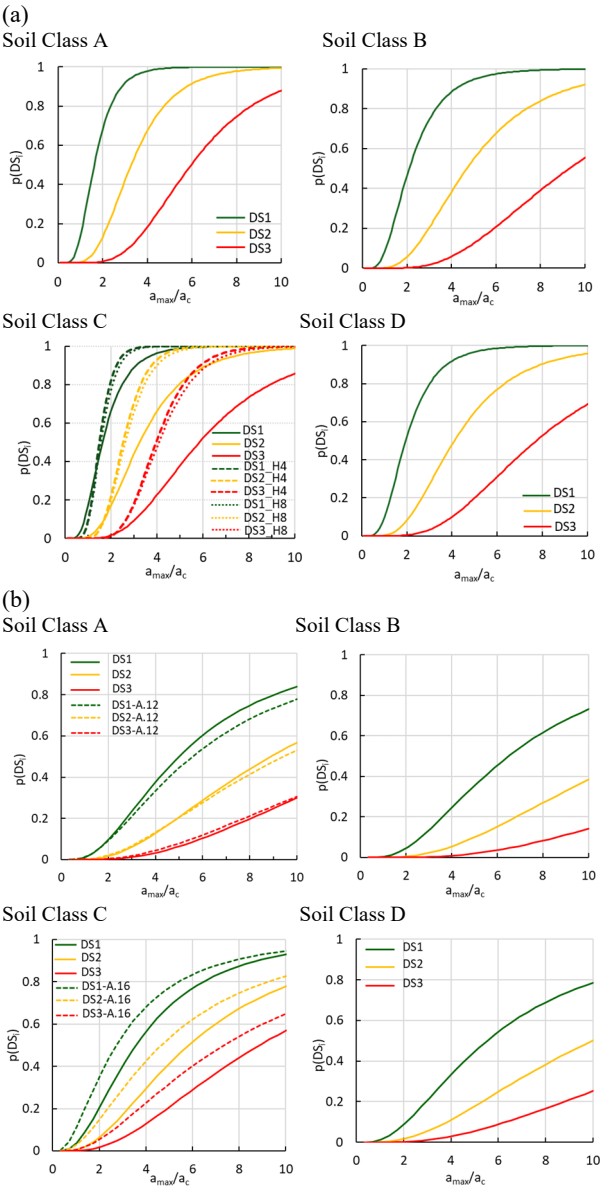

Figure 8. Comparison of fragility curves for retaining walls (a) and embankments (b).

Figure 9 and Figure 10 show the resulting functionality loss curves. The functions in Figure 9 and Figure 10 allow to individuate the functionality loss level directly from the intensity measure of the ground motion. They turn out to be useful in the resilience assessment of road networks, because the actions that limit the road fruition are known, once the shake maps of just occurred or expected earthquakes are available.

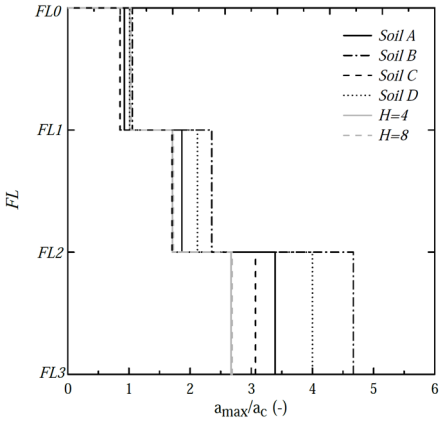

Figure 9. Functionality loss of retaining walls.

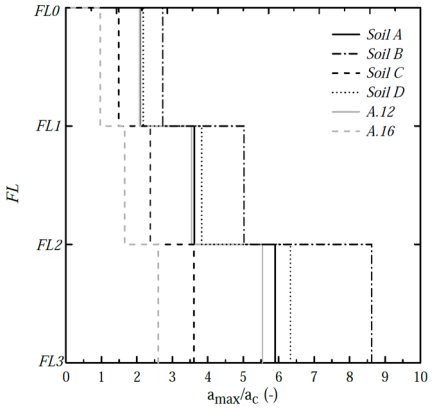

Figure 10. Functionality loss of embankments.

5 VALIDATION AGAINST CASE STUDIES

The reliability of the fragility curves in Figure 8 was assessed through application to two case studies of embankments and two case studies of retaining walls.

The first embankment, located along the A16 Napoli-Canosa highway, is 7.60 m high with a slope of 29° (see Figure 2). The embankment is composed of gravel, while the subsoil consists of three distinct layers: the first (8-12 m) and the second (12-18 m) are silty soils with comparable strength and stiffness parameters, whereas the third layer (18-30 m) consists of clayey soils. Figure 11 shows the physical and mechanical parameters used in this study. In lack of more specific data, the bedrock was assumed at a depth of 30 m, resulting in an equivalent shear wave velocity (V_S) of 347 m/s, corresponding to soil class C. Further details are provided in Dionisio et al. (2025).

The second embankment is located along the A12 Roma-Civitavecchia-Tarquinia highway. At its most critical section, the embankment reaches a height of 22 m and a slope of 28° on the left carriageway. It is founded on a limestone formation and mainly composed of fine-grained soils, which have caused continuous settlements over time. Site investigations revealed that the embankment is relatively homogeneous. Figure 12

summarizes the parameters used in this study, with additional details available in Dionisio et al. (2025).

The critical accelerations for each embankment, obtained through numerical modeling, are 0.34g for the A16 embankment and 0.024g for the A12 embankment, confirming the latter's low static stability. In both cases, the critical failure mechanism is sliding along a logarithmic spiral surface.

Displacements were calculated using nonlinear dynamic analyses performed on two-dimensional numerical models with the finite difference code FLAC. The mechanical behavior of the soils was simulated through a nonlinear, hysteretic constitutive model with a Mohr-Coulomb failure criterion.

The two retaining walls analyzed are 8 m and 4 m high, respectively. Both walls are founded on a homogeneous 40 m-thick clay layer, where V_S increases with depth according to the correlation proposed by d'Onofrio and Silvestri (2001), resulting in an equivalent velocity of 200 m/s down to the bedrock. The selected soil profile falls under class C. The unit weight of the soil was assumed to be 20 kN/m³, while the undrained shear strength was set to 80 kPa, in agreement with the V_S of the upper 5 meters, based on the correlation proposed by Mayne e Rix (1995). The geometric properties of the two walls were defined by simulating their design according to the Italian Building Code (DM, 2001), considering their height, the mechanical properties of the foundation soil, and a backfill friction angle $\varphi = 35°$. The critical acceleration of the taller wall is 0.15g and corresponds to a sliding failure mechanism, while for the shorter wall, the most critical mechanism is the foundation bearing capacity, with $a_c = 0.26$g.

The fragility curves for the two retaining walls were computed using the same procedure described in Section 2, but the input motions applied to the walls resulted from equivalent-linear site response analyses. These were performed using the STRATA code, considering a set of 320 ground motions recorded on rock outcrop with flat topography (see Brunelli et al. (2025)). The nonlinear and dissipative behavior of the clay was simulated using the model calibrated by Ciancimino et al. (2020) on resonant column test data from central Italy soils.

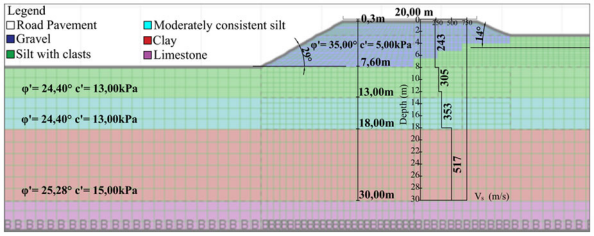

Figure 11. Embankment along the A.16 highway with indication of physical and mechanical properties.

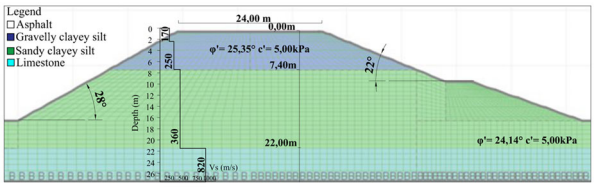

Figure 12. Embankment along the A.12 highway with indication of physical and mechanical properties.

Figure 13 and Figure 14 compare the mean damage for retaining walls (Figure 13) and embankments (Figure 14), defined using the following equation:

$$\mu = \sum_{i=1}^{3} iP(DS_i) \tag{3}$$

which represents a weighted average over the index i of the probability of failure $P(DS_i)$. The latter is obtained from the fragility curves derived using the generalized approach to calculate the μ values shown on the x-axis in Figure 13 and Figure 14, and from the case-specific fragility curves to obtain the y-axis values, under the same a_{max}/a_c ratio and soil type.

The damage estimates produced using the generalized approach show very good agreement with those derived from the case studies, especially for embankments, demonstrating the effectiveness of the proposed methodology.

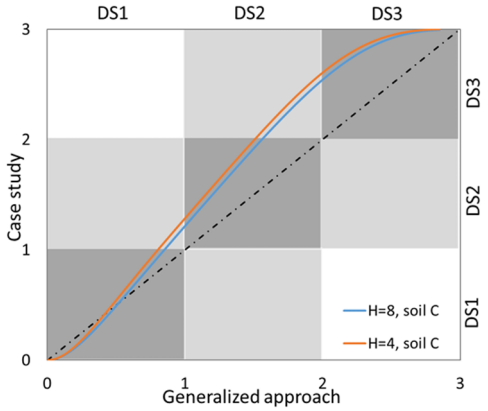

Figure 13. Comparison between mean damage curves obtained using fragility curves from the generalized approach and from single case studies for retaining walls.

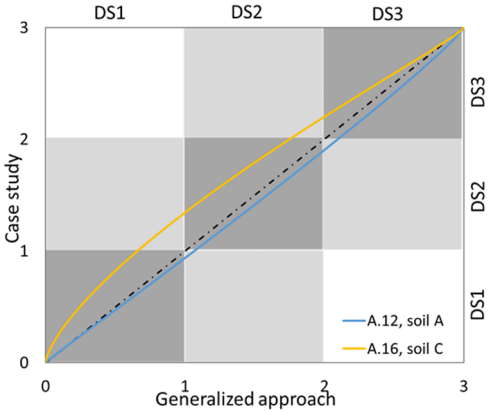

Figure 14. Comparison between mean damage curves obtained using fragility curves from the generalized approach and from single case studies for embankments.

6 CONCLUSIONS

This work presents and discusses the derivation of fragility curves for classes of embankments and retaining walls along the Italian highway network. Despite the wide variability in the considered parameters, including the subsoil type of the seismic input, height, acceleration, and slope (for embankments), the trend of displacements as a function of the maximum acceleration normalized with respect to the critical acceleration of the system appears to be predominantly governed by subsoil type of seismic input. This behavior is since the displacement thresholds used to define damage fall within the plateau region of the capacity curves and are therefore influenced solely by the critical acceleration.

This key observation allows the development of fragility curves that are applicable to all walls and embankments located on soils of the same classification. The application of the

method to four case studies has confirmed the effectiveness of the proposed approach.

7 ACKNOWLEDGEMENTS

The research activities discussed in the paper were funded by the European Union - Next Generation EU, M4C2 mission of the Italian National Recovery and Resilience Plan, investment 1.1-, through the research project of relevant national interest *Framework to Assess the Infrastructure Resilience and Management Operations In Roads After Earthquake*, *FAIR MOIRAE* (Project Code: P202224T7S).

8 REFERENCES

Amendola, C., Conti, R., de Silva, F. 2025. Curve di fragilità e perdita di funzionalità di opere di sostegno in sistemi infrastrutturali di trasporto*". 28° Convegno Nazionale di Geotecnica,* Italia.

Callisto, L. 2019. On the seismic design of displacing earth retaining systems. *EarthProc. 7th International Conference on Earthquake Geotechnical Engineering*, Italy, 239–255.

Ciancimino, A., Lanzo, G., Alleanza, G. A., et al. 2020. Dynamic characterization of fine-grained soils in Central Italy by laboratory testing. *Bulletin of Earthquake Engineering* 18, 5503–5531.

Cosentini, R. M., Bozzoni, F. 2022. Fragility curves for rapid assessment of earthquake-induced damage to earth-retaining walls starting from optimal seismic intensity measures. *Soil Dynamics and Earthquake Engineering* 152 (6).

Dionisio, F., Caiafa, F., de Silva, F., Conti R. 2025. Validazione degli approcci semplificati per la costruzione delle curve di fragilità di rilevati stradali attraverso due casi studio. *28° Convegno Nazionale di Geotecnica*, Italia.

d'Onofrio, A., Silvestri, F. 2001. Influenza della microstruttura sulla rigidità a piccola deformazione e sullo smorzamento del suolo a grana fine ed effetti sulla risposta locale del sito. *Conferenze internazionali sui recenti progressi nell'ingegneria sismica geotecnica e nella dinamica del suolo.*

Jalayer, F., De Risi, R., Manfredi, G. 2015. Bayesian Cloud Analysis: efficient structural fragility assessment using linear regression. *Bulletin of Earthquake Engineering* 13, 1183-1203.

Kaynia, M.A., Argyroudis, S., Mayoral, J.M., Johansson, J., Pitilakis, K., Anastasiadis, A. 2011. D3.7: fragility functions for roadway system elements. *Report for the European Project SYNER-G: Systemic Seismic Vulnerability and Risk Analysis for Buildings, Lifeline Networks and Infrastructures Safety Gain* (FP7-ENV-2009-1-244061).

Mayne, Paul W., Rix, Glenn J. 1995. Correlations between shear wave velocity and cone tip resistance in natural clays. *Soils and foundations* 35 (2), 107-110,

National Institute of Building Science (NIBS) 1999. HAZUS99 technical manual, developed by the Federal Emergency Management Agency, Washington, D.C.

Stokoe, K. H., II, Darendeli, M. B., Rathje, E. M., Roblee, C. J. 2001. Development of a New Family of Normalized Modulus Reduction and Material Damping Curves. ASCE Journal of Geotechnical Engineering, 119(11), 1805–1822.

Vucetic, M., Dobry, R. 1991. Effect of soil plasticity on cyclic response. *Journal of Geotechnical Engineering* 117:1(89)

Zeolla, E., Brunelli, A., de Silva, F., Cattari, S., Sica, S. 2025. Fragility curves of URM buildings in aggregate considering the interaction with soil and among nearby footings. *Bulletin of Earthquake Engineering*, 23(9), 3589-3622.